

# Recent *BABAR* results on measurement of exclusive hadronic cross sections

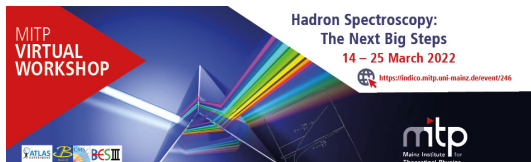


Evgeny Solodov  
representing the *BABAR* Collaboration



BudkerINP and Novosibirsk State University  
[solodov@inp.nsk.su](mailto:solodov@inp.nsk.su)

Hadron Spectroscopy: The Next Big Step  
MITP virtual workshop



# Outline

- New precision measurement of  $e^+e^- \rightarrow \pi^+\pi^-\pi^0$  cross section  
Phys.Rev.D 104, 112003 (2021)
- First measurements of  $e^+e^- \rightarrow \pi^+\pi^-4\pi^0$  and  
 $e^+e^- \rightarrow \pi^+\pi^-3\pi^0\eta$  cross sections  
Phys.Rev.D 104, 112004 (2021)
- First measurements of  $e^+e^- \rightarrow 2(\pi^+\pi^-)3\pi^0$  and  
 $e^+e^- \rightarrow 2(\pi^+\pi^-)2\pi^0\eta$  cross sections  
Phys.Rev.D 103, 092001 (2021)



# $a_\mu = \frac{1}{2}(g - 2)_\mu$ precision test of SM

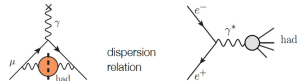
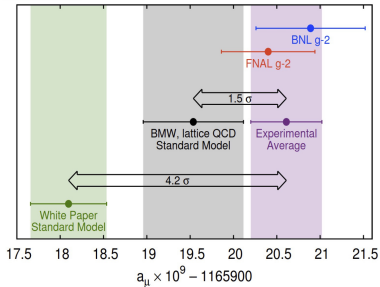
SM prediction for muons:

$$a_\mu = a_\mu^{QED} + a_\mu^{EW} + a_\mu^{hadr}$$

absolute value dominated by  $a_\mu^{QED} + a_\mu^{EW}$

ERROR dominated by  $a_\mu^{hadr}$ : not calculable perturbatively

$a_\mu^{hadr}$ : LQCD or data-driven dispersive approach



$K(s)$ : analytically known kernel function

$$a_\mu^{had, LO} = \frac{\alpha^2(0)}{3\pi^2} \int_{4m_\pi^2}^{\infty} ds \frac{K(s)}{s} R(s)$$

$$R(s) = \frac{\sigma(e^+e^- \rightarrow \text{hadrons})}{\sigma(e^+e^- \rightarrow \mu^+\mu^-)} \text{ experimental input}$$

relies on hadronic cross section measurements

4.2  $\sigma$  (WP/SM) or 1.5  $\sigma$  (LQCD/SM)

Largest contribution to the integral from hadronic cross section at low energies

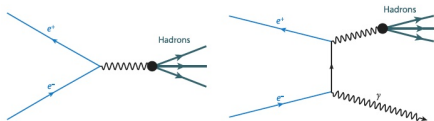
For  $\sqrt{s} \lesssim 2 \text{ GeV}$  finite number of final states contribute:

$\sigma(e^+e^- \rightarrow \text{hadrons})$  can be obtained as sum of all exclusive cross sections



# BABAR hadronic cross section measurements using ISR

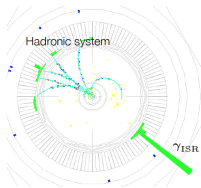
Initial State Radiation from  $e^+e^-$  allows to measure cross sections at all center-of-mass energies  $\sqrt{s'}$  below the nominal  $\sqrt{s}$  of the beams:



$$\frac{d\sigma(s; s'; \theta_\gamma)}{ds' d\theta_\gamma} = W(s; s'; \theta_\gamma) \cdot \sigma_X(s')$$

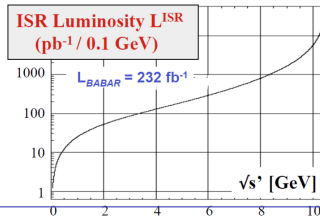
boost  $\Rightarrow$  harder momentum spectrum for daughter particles

tag photon to identify ISR events

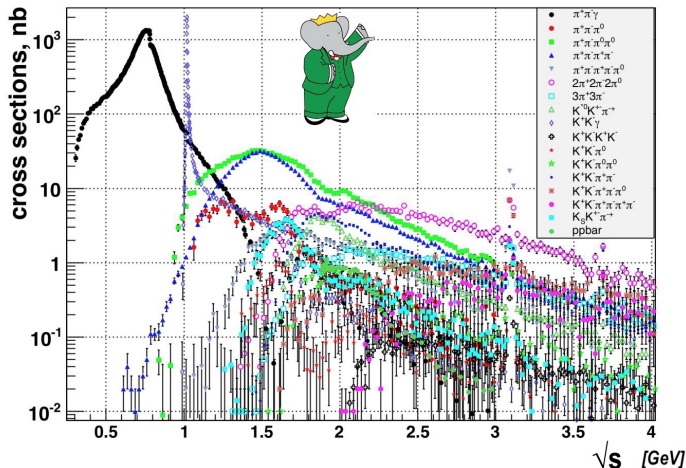


- hadrons in fiducial detector region
- fully reconstruct the final state
- kinematic fit: energy resolution

- cross sections down to threshold
- measure  $\sigma$  at all  $\sqrt{s}$  simultaneously
- large "effective" luminosity



# Light hadrons cross sections measured by *BABAR*



# Light hadrons cross sections measured in ISR by *BABAR*

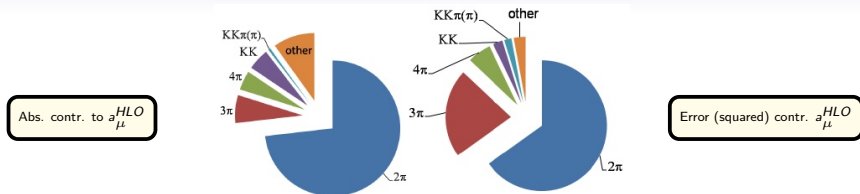
Many **first measurements**: (superseded results omitted)

$\pi^+\pi^-\pi^0$	469 fb <sup>-1</sup>	Phys. Rev. D 104, 112003 (2021)
$\pi^+\pi^-\pi^0\pi^0\pi^0$ and $\pi^+\pi^-\pi^0\pi^0\pi^0\eta$	469 fb <sup>-1</sup>	Phys. Rev. D 104, 112004 (2021)
$2(\pi^+\pi^-\pi^0\pi^0\pi^0)$ and $2(\pi^+\pi^-\pi^0\pi^0\eta)$	469 fb <sup>-1</sup>	Phys. Rev. D 103, 092001 (2021)
$\pi^+\pi^-\pi^0\pi^0\pi^0$ and $\pi^+\pi^-\pi^0\pi^0\eta$	469 fb <sup>-1</sup>	Phys. Rev. D 98, 112015 (2018)
$\pi^+\pi^-\eta$	469 fb <sup>-1</sup>	Phys. Rev. D 97, 052007 (2018)
$\pi^+\pi^-\pi^0\pi^0$	454 fb <sup>-1</sup>	Phys. Rev. D 96, 092009 (2017)
$K_S^0 K^\pm \pi^\mp \pi^0$ and $K_S^0 K^\pm \pi^\mp \eta$	454 fb <sup>-1</sup>	Phys. Rev. D 95, 092005 (2017)
$K_S^0 K_L^0 \pi^0$ , $K_S^0 K_L^0 \eta$ , and $K_S^0 K_L^0 \pi^0 \pi^0$	469 fb <sup>-1</sup>	Phys. Rev. D 95, 052001 (2017)
$K^+ K^-$ ( $\gamma$ undetected)	469 fb <sup>-1</sup>	Phys. Rev. D 92, 072008 (2015)
$K_S^0 K_L^0$ , $K_S^0 K_L^0 \pi^+ \pi^-$ , $K_S^0 K_S^0 \pi^+ \pi^-$ , and $K_S^0 K_S^0 K^+ K^-$	469 fb <sup>-1</sup>	Phys. Rev. D 89, 092002 (2014)
$K^+ K^-$	232 fb <sup>-1</sup>	Phys. Rev. D 88, 032013 (2013)
$\rho\bar{\rho}$	469 fb <sup>-1</sup>	Phys. Rev. D 87, 092005 (2013)
$\rho\bar{\rho}$ ( $E_{cm} : 3.0 \div 6.5$ GeV)	469 fb <sup>-1</sup>	Phys. Rev. D 88, 072009 (2013)
$\pi^+\pi^-\pi^+\pi^-$	454 fb <sup>-1</sup>	Phys. Rev. D 85, 112009 (2012)
$K^+ K^- \pi^+ \pi^-$ , $K^+ K^- \pi^0 \pi^0$ , and $K^+ K^- K^+ K^-$	454 fb <sup>-1</sup>	Phys. Rev. D 86, 012008 (2012)
$\pi^+ \pi^-$	232 fb <sup>-1</sup>	Phys. Rev. Lett. 103, 231801 (2009)
$K^+ K^- \eta$ , $K^+ K^- \pi^0$ and $K_S^0 K^\pm \pi^\mp$	232 fb <sup>-1</sup>	Phys. Rev. D 77, 092002 (2008)
$\Lambda\bar{\Lambda}$ , $\Lambda\bar{\Sigma}^0$ , and $\Sigma^0\bar{\Sigma}^0$	230, fb <sup>-1</sup>	Phys. Rev. D 76, 092006 (2007)
$2(\pi^+\pi^-)\pi^0$ , $2(\pi^+\pi^-)\eta$ , $K^+ K^- \pi^+ \pi^- \pi^0$ and $K^+ K^- \pi^+ \pi^- \eta$	232 fb <sup>-1</sup>	Phys. Rev. D 76, 092005 (2007)
$3(\pi^+\pi^-)$ , $2(\pi^+\pi^- \pi^0)$ and $K^+ K^- 2(\pi^+\pi^-)$	232 fb <sup>-1</sup>	Phys. Rev. D 73, 052003 (2006)



$$e^+e^- \rightarrow \pi^+\pi^-\pi^0$$

It gives the second largest contribution to  $a_\mu^{HLO}$  and its error



Previous *BABAR* measurement based on 20% of dataset available now  
Cross section had been measured in  $1.05 \div 3$  GeV

PRD 70, 072004 (2004)

New measurement using the whole dataset extends cross section below 1.05 GeV, in the region of  $\rho$ ,  $\omega$  and  $\phi$  resonances

accuracy on  $a_\mu^{HLO}$  contribution due to  $e^+e^- \rightarrow \pi^+\pi^-\pi^0$  currently  $\approx 3\%$   
new measurement will improve accuracy to  $\approx 1.5\%$



$$e^+e^- \rightarrow \pi^+\pi^-\pi^0\gamma_{ISR}$$

Detect all final state particles

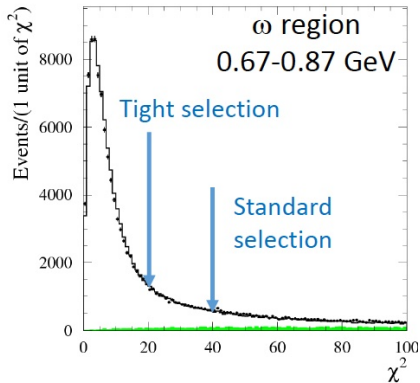
Select events using kinematic fit (cut on  $\chi^2$ )

Several additional cuts reduce background by factor 2

Remaining ISR and  $q\bar{q}$  background subtracted using simulation normalized to data.

Above 1.1 GeV sizeable FSR background from  $e^+e^- \rightarrow a_1\gamma, a_2\gamma$  processes.

Estimated by pQCD with 100% uncertainty.  
up to 8% contribution near 1.3 GeV

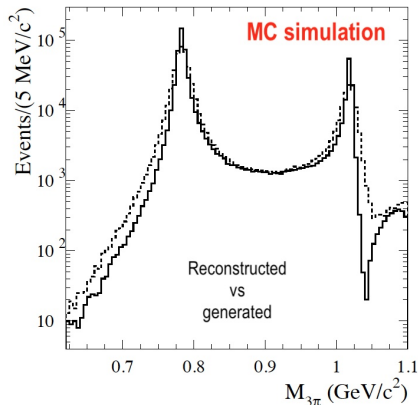


# $\pi^+\pi^-\pi^0$ mass spectrum below 1.1 GeV

Below 1.1 GeV the mass spectrum has a sharp structure

unfolding required to determine true spectrum

cross section result depends on the assumed mass resolution



The  $\omega$  and  $\phi$  widths are well known

⇒ use data to correct the simulated resolution function

Tails of the resolution depend on the  $\chi^2$  cut applied in selecting events:

⇒ try more than one cut value



# Fit to the $\pi^+\pi^-\pi^0$ mass spectrum

The mass spectrum fitted with VDM model including

$\omega(782) + \omega(1420) + \omega(1680) + \phi(1020)$  resonances

$\omega(782)$  and  $\phi$  widths fixed to PDG average

+ the rare  $\rho(770) \rightarrow 3\pi$  decay

For  $\chi^2 < 20$  (nominal fit) the mass spectrum is well described by introducing an additional Gaussian smearing to the MC resolution function

$\sigma_s = 1.5 \pm 0.2$  MeV

$m_\omega - m_{PDG} = 0.042 \pm 0.055$  MeV

$m_\phi - m_{PDG} = 0.095 \pm 0.084$  MeV

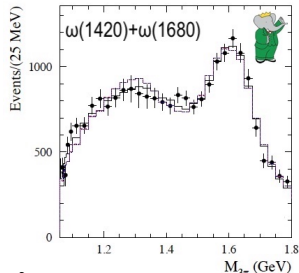
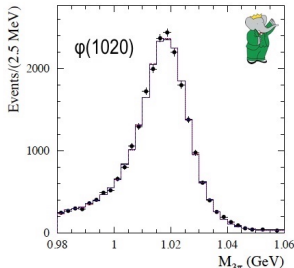
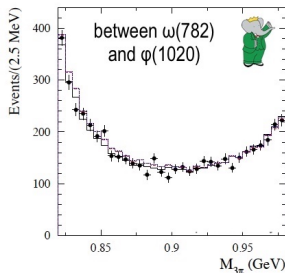
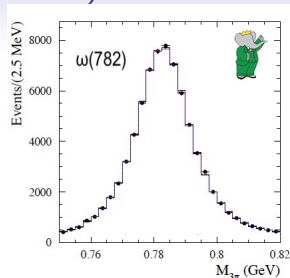
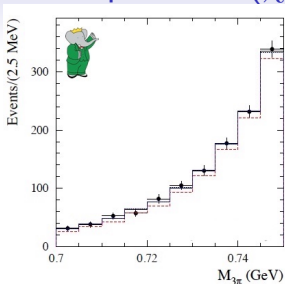
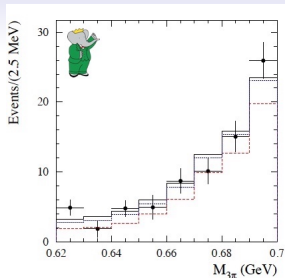
For  $\chi^2 < 40$  (cross check): additional Lorentzian smearing required to describe tails  
 $fraction = 0.7 \pm 0.2\%$ ;  $\gamma = 63 \pm 35$  GeV

consistent results for all other parameters

The data spectrum CANNOT be adequately described with  $\mathcal{B}(\rho \rightarrow 3\pi) \equiv 0$



# Fits to the $\pi^+\pi^-\pi^0$ mass spectrum ( $\chi^2 < 40$ )



- (solid): Lorentzian smearing and  $\rho \rightarrow 3\pi$   
 (dash): No Lorentzian smearing and no  $\rho \rightarrow 3\pi$   
 (dot): Lorentzian smearing and no  $\rho \rightarrow 3\pi$

$$\chi^2/\nu = 136/127$$

$$\chi^2/\nu = 201/131$$

$$\chi^2/\nu = 180/129$$



## Fit results on resonance parameters

For  $\omega(782)$  and  $\phi(1020)$  the products  $\Gamma_{ee} \times \mathcal{B}_{3\pi}$  are in reasonable agreement with world average values:

$$\Gamma(\omega \rightarrow e^+e^-) \cdot \mathcal{B}(\omega \rightarrow \pi^+\pi^-\pi^0) = (0.5698 \pm 0.0031 \pm 0.0082) \text{ keV}$$

world average:  $(0.557 \pm 0.011) \text{ keV}$

$$\Gamma(\phi \rightarrow e^+e^-) \cdot \mathcal{B}(\phi \rightarrow \pi^+\pi^-\pi^0) = (0.1841 \pm 0.0021 \pm 0.0080) \text{ keV}$$

world average:  $(0.1925 \pm 0.0043) \text{ keV}$

The rare decay  $\rho \rightarrow \pi^+\pi^-\pi^0$  is observed with significance greater than  $6\sigma$  the value and the relative phase wrt to the  $\omega(782)$  amplitude are in agreement with the only previous measurement by SND

SND: Phys.Rev.D 63,07002 (2001)

$$\mathcal{B}(\rho \rightarrow \pi^+\pi^-\pi^0) = (0.88 \pm 0.23 \pm 0.30) \times 10^{-4}$$

SND:  $(1.01^{+0.54}_{-0.34} \pm 0.34) \times 10^{-4}$

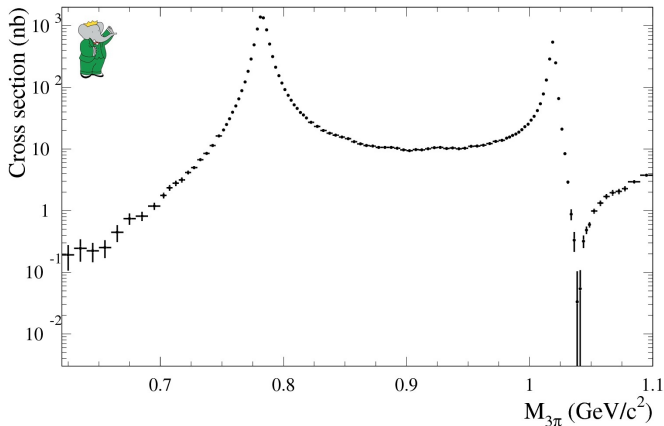
$$\phi_\rho - \phi_\omega = -(99 \pm 9 \pm 15)^\circ$$

SND:  $-(135^{+17}_{-13} \pm 9)^\circ$



# $e^+e^- \rightarrow \pi^+\pi^-\pi^0$ cross section below 1.1 GeV

The parameters of the smearing function determined in the VDM fit are used to correct the simulated resolution function



The unfolding is performed using the IDS (iterative dynamically stabilized) method (B. Malaescu, arXiv:0907.3791)

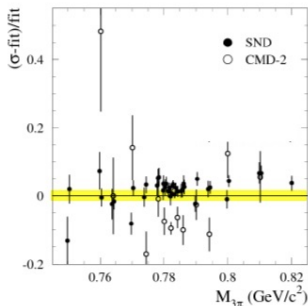
Systematic uncertainty at  $\omega(782)$  and  $\phi(1020)$  peak  $\approx 1.3\%$



# $e^+e^- \rightarrow \pi^+\pi^-\pi^0$ cross section below 1.1 GeV: comparison with previous measurements

SND: Phys.Rev.D 68,052006 (2003)

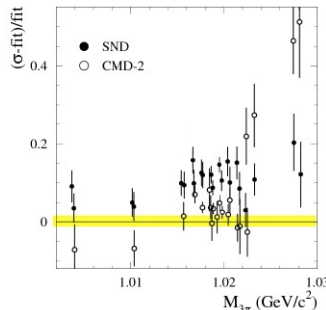
CMD-2: Phys.Lett.B 578,285 (2004)



SND-*BABAR* difference  $\simeq 2\%$   
below syst. (3.4% SND, 1.4% *BABAR*)  
CMD-2 (1.8% stat and 1.3% syst) is  
 $\simeq 7\%$  smaller than *BABAR*  
 $\simeq 2.7\sigma$  difference

SND: Phys.Rev.D 63,072002 (2001)

CMD-2: Phys.Lett.B 642,203 (2006)

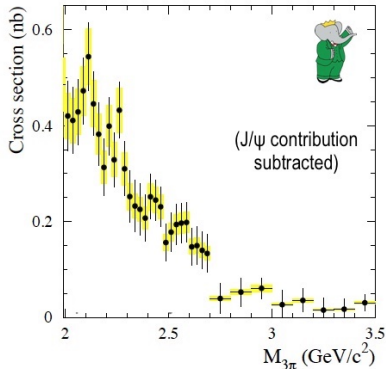
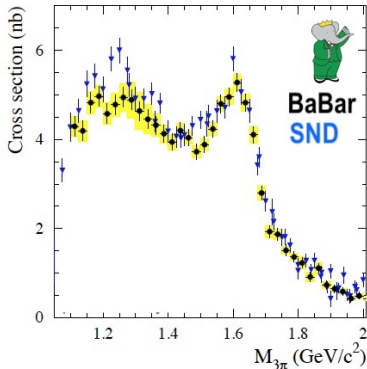


SND-*BABAR* difference  $\simeq 11\%$   
syst: 5% (SND); 1.4% (*BABAR*)  
CMD-2-*BABAR* difference  $\simeq 3\%$   
syst: 2.5% (CMD-2); 1.4% (*BABAR*)



# $e^+e^- \rightarrow \pi^+\pi^-\pi^0$ cross section above 1.1 GeV

No smearing is needed above 1.1 GeV. Syst. uncertainty:  $4 \div 15\%$   
dominated by background subtraction



Significant localized differences around 1.25 GeV and 1.5 GeV between *BABAR* and SND (Eur.Phys.J. C 80, 993 (2020))



# Impact on $a_\mu^{3\pi}$

$M_{3\pi} \text{ GeV}/c^2$	$a_\mu^{3\pi} \times 10^{10}$
0.62–1.10	$42.91 \pm 0.14 \pm 0.55 \pm 0.09$
1.10–2.00	$2.95 \pm 0.03 \pm 0.16$
$< 2.00$	$45.86 \pm 0.14 \pm 0.58$
$< 1.80$ [A]	$46.21 \pm 0.40 \pm 1.40$
$< 1.97$ [B]	$46.74 \pm 0.94$
$< 2$ [C]	$44.32 \pm 1.48$

[A] M. Davier, A. Hoecker, B. Malaescu and Z. Zhang, Eur.Phys.J. C 80, 241 (2020)

[B] A. Keshavarzi, D. Nomura and T. Teubner, Phys.Rev.D 101, 014029 (2020)

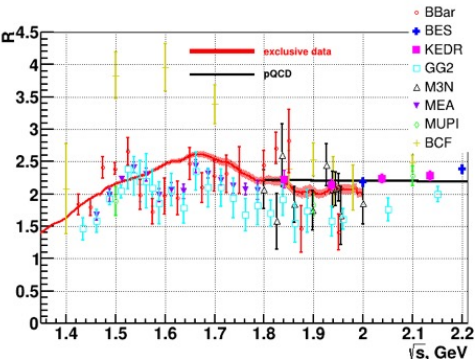
[C] F. Jegerlehner, Springer Tracts Mod. Phys. 274, 1 (2017)

The value of  $a_\mu^{3\pi}$  calculated using the  $e^+e^- \rightarrow \pi^+\pi^-\pi^0$  cross-section is in reasonable agreement with earlier calculations

the error on this contribution is reduced by a factor  $\approx 2$



# Is anything still missing?



Because of large, highly segmented calorimeter BaBar has advantage for study of the multi-photon reactions over detectors at VEPP2000 (SND and CMD-3) even effective integrated luminosity is already lower. It was demonstrated for the study of the  $e^+e^- \rightarrow \pi^+\pi^-\pi^0\pi^0\pi^0$ ,  $\pi^+\pi^-\pi^0\pi^0\eta$  reactions [Phys.Rev.D 98, 112015 \(2018\)](#).

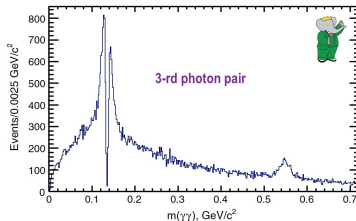
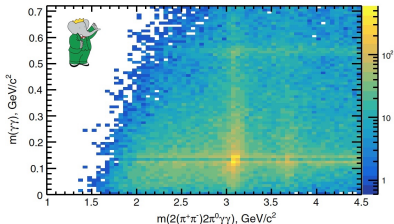
Currently, the sum of exclusive cross sections near 2.0 GeV shows a systematic deviation from the QCD predictions. BABAR, SND and CMD-3 measurements of previously unmeasured processes, e.g.

$e^+e^- \rightarrow \pi^+\pi^-\pi^0\pi^0\pi^0\pi^0$ ,  $\pi^+\pi^-\pi^+\pi^-\pi^0\pi^0\pi^0$ ,  $K_S K^\pm \pi^\mp \pi^0\pi^0$ ,  $K^- K^+ \pi^0\pi^0\pi^0$ , ... may help to understand if this deviation is real.

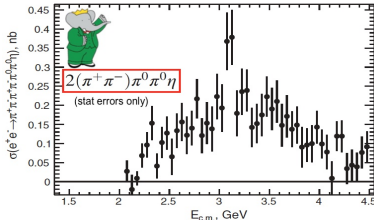
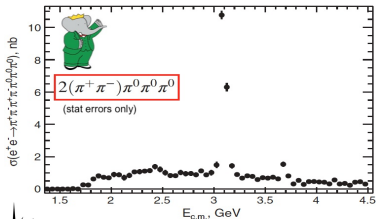


$$e^+e^- \rightarrow 2(\pi^+\pi^-)3\pi^0 \text{ and } 2(\pi^+\pi^-)2\pi^0\eta \text{ (first measurement)}$$

All candidate events with 4 oppositely charged tracks, one  $\gamma_{ISR}$  photon candidate, 2 photon pairs with  $m_{\gamma\gamma}$  compatible with  $\pi^0$  and a third photon pair + kinematic fit. Signal events selected based on  $\chi^2 < 50$ ; background from  $\chi^2$  sidebands. + some additional cuts to reduce background.

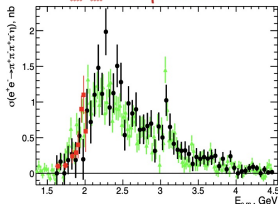


Fit the third photon pair mass distribution in bins of  $m(2(\pi^+\pi^-)2\pi^0\gamma\gamma)$  to determine the  $2(\pi^+\pi^-)3\pi^0$  and  $2(\pi^+\pi^-)2\pi^0\eta$  yields to determine cross sections



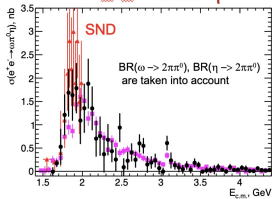
# Intermediate states in $e^+e^- \rightarrow 2(\pi^+\pi^-)3\pi^0$

$$e^+e^- \rightarrow \eta\pi^+\pi^-\pi^+\pi^-$$



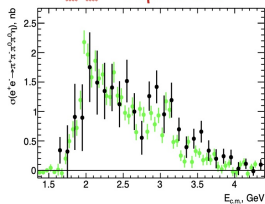
BaBar  $\eta \rightarrow \gamma\gamma$  (Phys.Rev. D76 (2007) 092005)  
CMD-3  $\eta \rightarrow \pi^+\pi^-\pi^0$  Phys.Lett. B792 (2019) 419-423

$$e^+e^- \rightarrow \omega\pi^0\eta$$



BaBar data for the  $e^+e^- \rightarrow \omega\pi^0\eta(\eta \rightarrow \gamma\gamma)$  reaction  
Phys.Rev. D98 (2018) no.11, 112015, and still are  
lower than SND measurement.

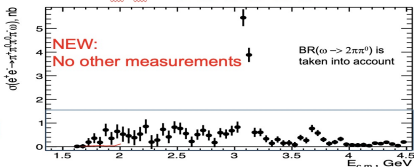
$$e^+e^- \rightarrow \eta\pi^+\pi^-\pi^0\pi^0$$



BaBar result for  $\eta \rightarrow \gamma\gamma$  mode  
Phys.Rev. D98 (2018) no.11, 112015

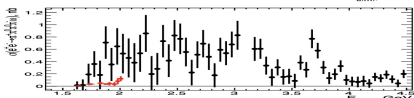
Good agreement with previously measured cross sections in different decay modes of  $\omega$ ,  $\eta$

$$e^+e^- \rightarrow \omega\pi^+\pi^-\pi^0\pi^0$$



Phys.Rev.D 103, 092001 (2021)

(not shown:  $\rho^\pm\pi^\mp\pi^+\pi^-2\pi^0$ )



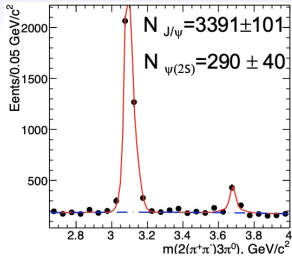
CMD-3 results are shown for the  $e^+e^- \rightarrow \omega\pi^+\pi^-\pi^+\pi^-$  reaction  
Phys.Lett. B792 (2019) 419-423

No significant evidence for other  
intermediate states



# $e^+e^- \rightarrow 2(\pi^+\pi^-)3\pi^0$ and $2(\pi^+\pi^-)2\pi^0\eta$ : charmonium

Phys.Rev.D 103, 092001 (2021)



Measured quantity	Measured value (eV)	Calculated, this work	PDG [22]
$\Gamma_{ee}^{J/\psi} \cdot \mathcal{B}_{J/\psi \rightarrow \pi^+ \pi^- \pi^+ \pi^- \pi^0 \pi^0 \pi^0}$	$345.0 \pm 10.0 \pm 50.0$	$62.0 \pm 2.0 \pm 9.0$	No entry
$\Gamma_{ee}^{J/\psi} \cdot \mathcal{B}_{J/\psi \rightarrow \omega \pi^+ \pi^- \pi^0 \pi^0} \cdot \mathcal{B}_{\omega \rightarrow \pi^+ \pi^- \pi^0}$	$165.0 \pm 9.0 \pm 25.0$	$33.0 \pm 2.0 \pm 5.0$	No entry
$\Gamma_{ee}^{J/\psi} \cdot \mathcal{B}_{J/\psi \rightarrow \eta \pi^+ \pi^- \pi^0 \pi^0} \cdot \mathcal{B}_{\eta \rightarrow \pi^+ \pi^- \pi^0}$	$6.0 \pm 4.0 \pm 1.0$	$4.8 \pm 3.2 \pm 0.8$	$2.3 \pm 0.5$
$\Gamma_{ee}^{J/\psi} \cdot \mathcal{B}_{J/\psi \rightarrow \pi^+ \pi^- \pi^+ \pi^- \eta} \cdot \mathcal{B}_{\eta \rightarrow \pi^0 \pi^0 \pi^0}$	$5.6 \pm 2.6 \pm 0.8$	$2.6 \pm 1.2 \pm 0.5$	$2.26 \pm 0.28$
$\Gamma_{ee}^{J/\psi} \cdot \mathcal{B}_{J/\psi \rightarrow \rho^+ \pi^- \pi^+ \pi^- \pi^0 \pi^0}$	$155.0 \pm 26.0 \pm 36.0$	$28.0 \pm 4.7 \pm 6.6$	No entry
$\Gamma_{ee}^{J/\psi} \cdot \mathcal{B}_{J/\psi \rightarrow \rho^+ \rho^- \pi^+ \pi^- \pi^0}$	$32.0 \pm 13.0 \pm 15.0$	$5.7 \pm 2.4 \pm 2.7$	No entry
$\Gamma_{ee}^{J/\psi} \cdot \mathcal{B}_{J/\psi \rightarrow \pi^+ \pi^- \pi^+ \pi^- \pi^0 \pi^0 \eta} \cdot \mathcal{B}_{\eta \rightarrow \gamma \gamma}$	$9.1 \pm 2.6 \pm 1.4$	$4.2 \pm 1.2 \pm 0.6$	No entry
$\Gamma_{ee}^{\psi(2S)} \cdot \mathcal{B}_{\psi(2S) \rightarrow \pi^+ \pi^- \pi^+ \pi^- \pi^0 \pi^0 \pi^0}$	$33.0 \pm 5.0 \pm 5.0$	$14.0 \pm 2.0 \pm 2.0$	No entry
$\Gamma_{ee}^{\psi(2S)} \cdot \mathcal{B}_{\psi(2S) \rightarrow J/\psi \pi^0 \pi^0} \cdot \mathcal{B}_{J/\psi \rightarrow \pi^+ \pi^- \pi^+ \pi^- \pi^0}$	$14.8 \pm 2.6 \pm 2.2$	$34.7 \pm 6.1 \pm 5.2$	$33.7 \pm 2.6$
$\Gamma_{ee}^{\psi(2S)} \cdot \mathcal{B}_{\psi(2S) \rightarrow J/\psi \pi^+ \pi^-} \cdot \mathcal{B}_{J/\psi \rightarrow \pi^+ \pi^- \pi^0 \pi^0 \pi^0}$	$19.2 \pm 4.5 \pm 3.2$	$23.8 \pm 5.6 \pm 3.6$	$27.1 \pm 2.9$
$\Gamma_{ee}^{\psi(2S)} \cdot \mathcal{B}_{\psi(2S) \rightarrow \omega \pi^+ \pi^- \pi^0 \pi^0} \cdot \mathcal{B}_{\omega \rightarrow \pi^+ \pi^- \pi^0}$	$18.0 \pm 4.0 \pm 3.0$	$8.7 \pm 1.9 \pm 1.5$	No entry
$\Gamma_{ee}^{\psi(2S)} \cdot \mathcal{B}_{\psi(2S) \rightarrow \pi^+ \pi^- \pi^+ \pi^- \pi^0 \pi^0 \eta} \cdot \mathcal{B}_{\eta \rightarrow \gamma \gamma}$	$< 1.9$ at 90% C.L.	$< 2.0$ at 90% C.L.	No entry
$\Gamma_{ee}^{\psi(2S)} \cdot \mathcal{B}_{\psi(2S) \rightarrow \pi^+ \pi^- \pi^+ \pi^- \pi^0 \pi^0 \eta} \cdot \mathcal{B}_{\eta \rightarrow \pi^0 \pi^0 \pi^0}$	$< 2.3$ at 90% C.L.	$< 2.4$ at 90% C.L.	$1.2 \pm 0.6$

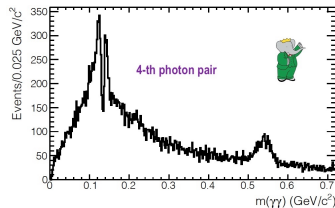
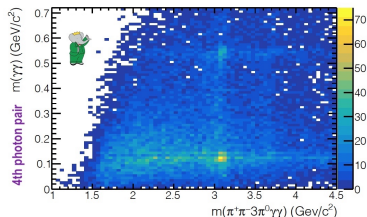


# $e^+e^- \rightarrow \pi^+\pi^-4\pi^0$ and $\pi^+\pi^-3\pi^0\eta$ (first measurement)

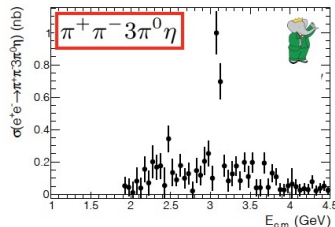
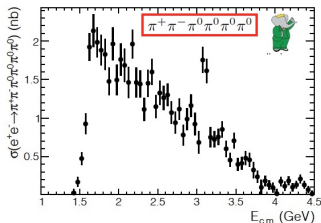
Events with 2 oppositely charged tracks, one  $\gamma_{ISR}$  photon candidate, 3 photon pairs with  $m_{\gamma\gamma}$  compatible with  $\pi^0$  and a fourth photon pair

Signal events selected based on  $\chi^2 < 70$ ; background from  $\chi^2$  sidebands

some additional cuts to reduce background



Fit the fourth photon pair invariant mass distribution in bins of  $m(\pi^+\pi^-3\pi^0\gamma\gamma)$  to determine the  $\pi^+\pi^-4\pi^0$  and  $\pi^+\pi^-3\pi^0\eta$  yields to determine cross sections



# Intermediate states in $e^+e^- \rightarrow \pi^+\pi^-\pi^0$

Intermediate states:

$$\pi^+\pi^-\pi^0\eta$$

$$\omega\eta$$

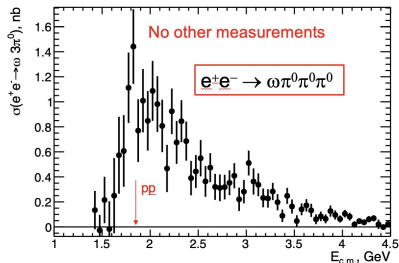
$$\omega 3\pi^0$$

$$(\rho\pi)3\pi^0$$

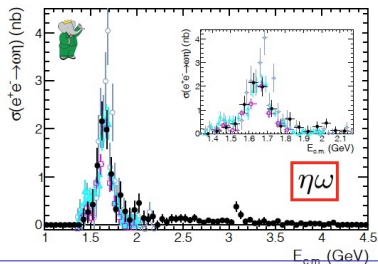
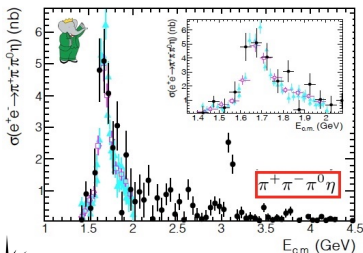
and possibly  $\rho^+\rho^-2\pi^0$

above 2.9 GeV

Sum of intermediate states seem to saturate the observed cross section

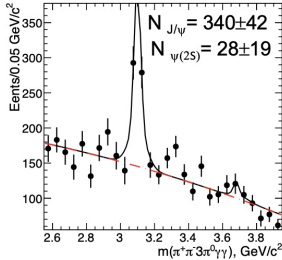


Below 2 GeV agreement with SND and CMD-2 measurements of  $\pi^+\pi^-\pi^0\eta$  and  $\omega\eta$ :



# $e^+e^- \rightarrow \pi^+\pi^-4\pi^0$ and $\pi^+\pi^-3\pi^0\eta$ : charmonium

Phys.Rev.D 104, 112003 (2021)



Measured Quantity	Measured Value (eV)	$J/\psi$ or $\psi(2S)$ Branching Fraction ( $10^{-3}$ ) Derived, this work	PDG [29]
$\Gamma_{ee}^{J/\psi} \cdot B_{J/\psi \rightarrow \pi^+\pi^-\pi^0\pi^0\pi^0}$	$35.8 \pm 4.4 \pm 5.4$	$6.5 \pm 0.8 \pm 1.0$	no entry
$\Gamma_{ee}^{J/\psi} \cdot B_{J/\psi \rightarrow \eta\pi^+\pi^-\pi^0} \cdot B_{\eta \rightarrow \pi^0\pi^0\pi^0}$	$21.1 \pm 1.7 \pm 3.2$	$11.9 \pm 0.9 \pm 2.3$	no entry
$\Gamma_{ee}^{J/\psi} \cdot B_{J/\psi \rightarrow \omega\eta} \cdot B_{\omega \rightarrow \pi^+\pi^-\pi^0} \cdot B_{\eta \rightarrow \pi^0\pi^0\pi^0}$	$4.9 \pm 2.1 \pm 0.7$	$3.0 \pm 1.3 \pm 0.5$	$1.74 \pm 0.20$
$\Gamma_{ee}^{J/\psi} \cdot B_{J/\psi \rightarrow \omega\pi^0\pi^0\pi^0} \cdot B_{\omega \rightarrow \pi^+\pi^-\pi^0}$	$9.4 \pm 2.3 \pm 1.5$	$1.9 \pm 0.5 \pm 0.3$	no entry
$\Gamma_{ee}^{J/\psi} \cdot B_{J/\psi \rightarrow \pi^+\pi^-\pi^0\pi^0\pi^0\eta} \cdot B_{\eta \rightarrow \gamma\gamma}$	$10.6 \pm 1.6 \pm 1.6$	$4.9 \pm 0.8 \pm 0.8$	no entry
$\Gamma_{ee}^{\psi(2S)} \cdot B_{\psi(2S) \rightarrow \pi^+\pi^-\pi^0\pi^0\pi^0\pi^0}$	$3.3 \pm 2.3 \pm 0.5$	$1.4 \pm 1.0 \pm 0.2$	no entry
$\Gamma_{ee}^{\psi(2S)} \cdot B_{\psi(2S) \rightarrow \eta\pi^+\pi^-\pi^0} \cdot B_{\eta \rightarrow \pi^0\pi^0\pi^0}$	$< 3.0$ at 90% C.L.	$< 3.5$ at 90% C.L.	no entry
$\Gamma_{ee}^{\psi(2S)} \cdot B_{\psi(2S) \rightarrow \omega\eta} \cdot B_{\omega \rightarrow \pi^+\pi^-\pi^0} \cdot B_{\eta \rightarrow \pi^0\pi^0\pi^0}$	$< 1.1$ at 90% C.L.	$< 1.4$ at 90% C.L.	$< 0.11$ at 90% C.L.
$\Gamma_{ee}^{\psi(2S)} \cdot B_{\psi(2S) \rightarrow \omega\pi^0\pi^0\pi^0} \cdot B_{\omega \rightarrow \pi^+\pi^-\pi^0}$	$< 1.6$ at 90% C.L.	$< 0.8$ at 90% C.L.	no entry
$\Gamma_{ee}^{\psi(2S)} \cdot B_{\psi(2S) \rightarrow \pi^+\pi^-\pi^0\pi^0\pi^0\eta} \cdot B_{\eta \rightarrow \gamma\gamma}$	$< 1.9$ at 90% C.L.	$< 2.0$ at 90% C.L.	no entry



# Conclusions

New measurement of the  $e^+e^- \rightarrow \pi^+\pi^-\pi^0$  cross section

Phys.Rev.D 104, 112003 (2021)

- based on the entire *BABAR* dataset
- measured in the range  $0.62 \div 3.5$  GeV
- 1.3% systematic uncertainty near the maxima of  $\omega(782)$  and  $\phi(1020)$
- the error on the leading order contribution to muon magnetic anomaly from  $e^+e^- \rightarrow \pi^+\pi^-\pi^0$  ( $E < 2$  GeV) reduced by a factor  $\approx 2$

First measurements of  $e^+e^- \rightarrow \pi^+\pi^-4\pi^0$  and  $e^+e^- \rightarrow \pi^+\pi^-3\pi^0\eta$  cross sections

Phys.Rev.D 104, 112004 (2021)

- The  $e^+e^- \rightarrow \pi^+\pi^-4\pi^0$  cross section seems to be saturated by intermediate states:  
 $\pi^+\pi^-\pi^0\eta$ ,  $\omega 3\pi^0$ ,  $(\rho\pi)3\pi^0$  and possibly  $\rho^+\rho^-2\pi^0$  intermediate states
- All possible combinations for the  $e^+e^- \rightarrow 6\pi$  cross section have been measured by *BABAR*-iso-spin relations are not needed for the HVP calculation.
- new  $J/\psi$  and  $\psi(2S)$  decay modes

First measurements of  $e^+e^- \rightarrow 2(\pi^+\pi^-)3\pi^0$  and  $e^+e^- \rightarrow 2(\pi^+\pi^-)2\pi^0\eta$  cross sections

Phys.Rev.D 103, 092001 (2021)

- The  $e^+e^- \rightarrow 2(\pi^+\pi^-)3\pi^0$  cross section seems to be saturated by intermediate states:  
 $2(\pi^+\pi^-)\eta$ ,  $\omega\pi^0\eta$ ,  $\rho^\pm\pi^\mp\pi^+\pi^-2\pi^0$ ,  $\eta\pi^+\pi^-2\pi^0$ ,  $\omega\pi^+\pi^-2\pi^0$
- new  $J/\psi$  and  $\psi(2S)$  decay modes



# BACKUP



# $a_\mu = \frac{1}{2}(g - 2)_\mu$ precision test of SM

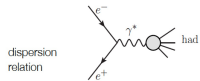
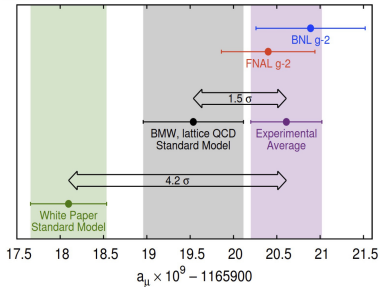
SM prediction for muons:

$$a_\mu = a_\mu^{QED} + a_\mu^{EW} + a_\mu^{hadr}$$

absolute value dominated by  $a_\mu^{QED} + a_\mu^{EW}$

ERROR dominated by  $a_\mu^{hadr}$ : not calculable perturbatively

$a_\mu^{hadr}$ : LQCD or data-driven dispersive approach



$K(s)$ : analytically known kernel function

$$a_\mu^{had, LO} = \frac{\alpha^2(0)}{3\pi^2} \int_{4m_\pi^2}^{\infty} ds \frac{K(s)}{s} R(s)$$

$$R(s) = \frac{\sigma(e^+e^- \rightarrow \text{hadrons})}{\sigma(e^+e^- \rightarrow \mu^+\mu^-)} \text{ experimental input}$$

4.2  $\sigma$  (WP/SM) or 1.5  $\sigma$  (LQCD/SM)

relies on hadronic cross section measurements

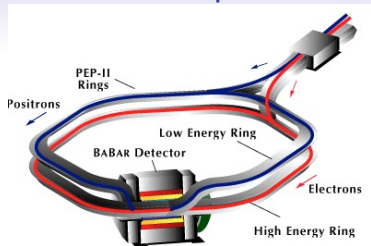
Largest contribution to the integral from hadronic cross section at low energies

For  $\sqrt{s} \lesssim 2 \text{ GeV}$  finite number of final states contribute:

$\sigma(e^+e^- \rightarrow \text{hadrons})$  can be obtained as sum of all exclusive cross sections



# The *BABAR* experiment



PEP-II **asymmetric  $e^+e^-$  collider** operating at center of mass energies near the  $\Upsilon(4S)$  (for most of the time)

$$\sqrt{s} = 10.58 \text{ GeV}/c^2$$

Asymmetric detector:

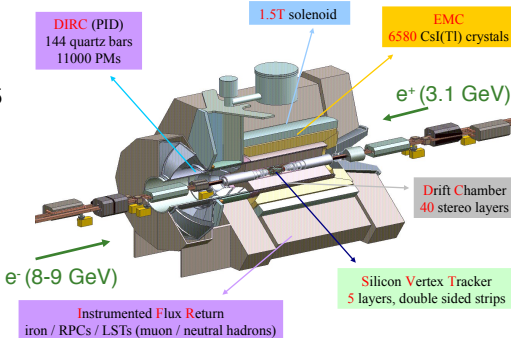
$$-0.9 < \cos \theta^* < 0.85$$

wrt electron beam

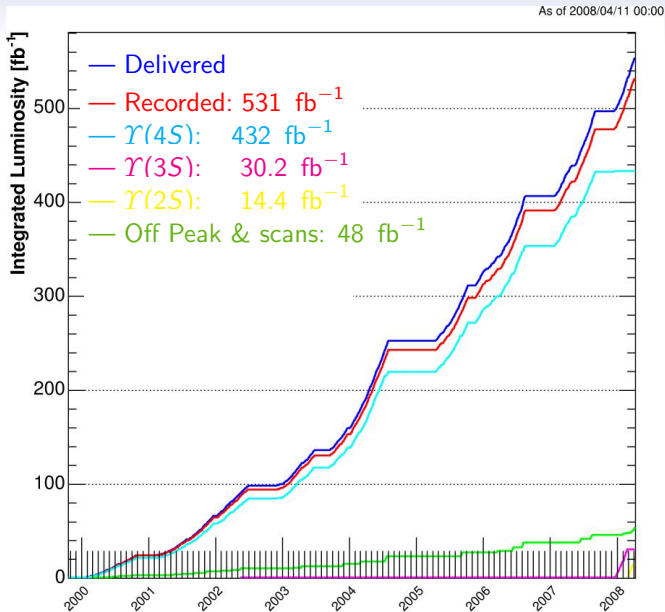
excellent performance:

- vertexing
- tracking
- PID
- calorimeter

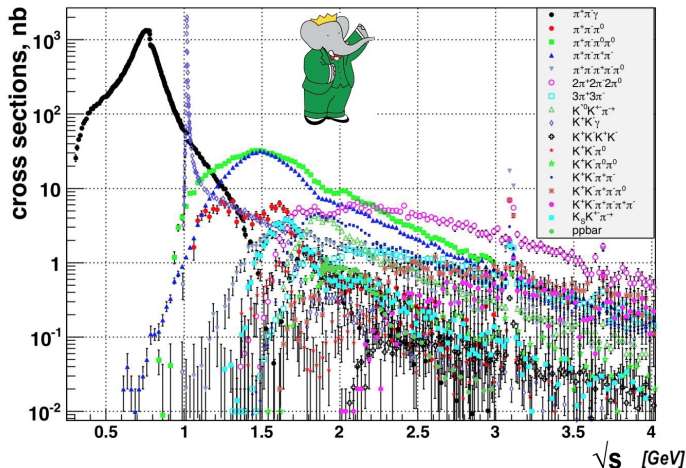
General-purpose detector



# Data samples



# Light hadrons cross sections measured by *BABAR*



# Substructures in $e^+e^- \rightarrow \pi^+\pi^-4\pi^0$

